

Video Article

The Synthesis, Characterization and Reactivity of a Series of Ruthenium *N*-triphos^{Ph} Complexes

Andreas Phanopoulos¹, Nicholas Long¹, Philip Miller¹
¹Department of Chemistry, Imperial College London

Correspondence to: Philip Miller at philip.miller@imperial.ac.uk

URL: <http://www.jove.com/video/52689>

DOI: [doi:10.3791/52689](https://doi.org/10.3791/52689)

Keywords: Chemistry, Issue 98, ligand, phosphine, coordination, complex, catalysis, ruthenium, biomass, levulinic acid

Date Published: 4/10/2015

Citation: Phanopoulos, A., Long, N., Miller, P. The Synthesis, Characterization and Reactivity of a Series of Ruthenium *N*-triphos^{Ph} Complexes. *J. Vis. Exp.* (98), e52689, doi:10.3791/52689 (2015).

Abstract

Herein we report the synthesis of a tridentate phosphine ligand $N(CH_2PPh_2)_3$ (*N*-triphos^{Ph}) (**1**) via a phosphorus based Mannich reaction of the hydroxylmethylene phosphine precursor with ammonia in methanol under a nitrogen atmosphere. The *N*-triphos^{Ph} ligand precipitates from the solution after approximately 1 hr of reflux and can be isolated analytically pure via simple cannula filtration procedure under nitrogen. Reaction of the *N*-triphos^{Ph} ligand with $[Ru_3(CO)_{12}]$ under reflux affords a deep red solution that show evolution of CO gas on ligand complexation. Orange crystals of the complex $[Ru(CO)_2\{N(CH_2PPh_2)_3\}-\kappa^3P]$ (**2**) were isolated on cooling to RT. The $^{31}P\{^1H\}$ NMR spectrum showed a characteristic single peak at lower frequency compared to the free ligand. Reaction of a toluene solution of complex **2** with oxygen resulted in the instantaneous precipitation of the carbonate complex $[Ru(CO_3)(CO)\{N(CH_2PPh_2)_3\}-\kappa^3P]$ (**3**) as an air stable orange solid. Subsequent hydrogenation of **3** under 15 bar of hydrogen in a high-pressure reactor gave the dihydride complex $[RuH_2(CO)\{N(CH_2PPh_2)_3\}-\kappa^3P]$ (**4**), which was fully characterized by X-ray crystallography and NMR spectroscopy. Complexes **3** and **4** are potentially useful catalyst precursors for a range of hydrogenation reactions, including biomass-derived products such as levulinic acid (LA). Complex **4** was found to cleanly react with LA in the presence of the proton source additive NH_4PF_6 to give $[Ru(CO)\{N(CH_2PPh_2)_3\}-\kappa^3P\{CH_3CO(CH_2)_2CO_2H\}-\kappa^2O](PF_6)$ (**6**).

Video Link

The video component of this article can be found at <http://www.jove.com/video/52689/>

Introduction

Ruthenium phosphine based complexes are some of the most widely studied and chemically versatile molecular catalysts.¹⁻⁹ Typically, such ruthenium catalysts contain either mono- or bi-dentate ligands that dictate the electronics, sterics, geometry and solubility of the complex, and which profoundly impact on catalytic activity. Multidentate phosphine systems have been less widely studied for catalysis, as they are known to impart greater stability on the metal center owing to the greater chelate effect of multiple phosphorus donors on the metal center. Such stabilization can be undesirable for catalysis, however, under harsher reaction conditions (higher temperatures and pressures) the complex stabilizing properties of such ligands can be advantageous in ensuring catalyst integrity. One such multidentate phosphine ligand system that we¹⁰⁻¹² and others¹³⁻¹⁸ have investigated for imparting complex stability and *facial* coordination geometries is the so-called *N*-triphos ligand series where three phosphine arms are attached to an apical bridging nitrogen atom forming a potentially tridentate ligand. One of the key features to these particular ligands is the facile way that they can be synthesized *via* a phosphorus based Mannich reaction from readily available secondary phosphines (**Figure 1**), hence phosphines with a variety of R-groups can be prepared usually in high yields and with minimal work-up. The overall goal of this methodology is to present a facile route by which ruthenium dihydride complexes featuring *N*-triphos ligands can be accessed for subsequent catalytic applications. Recently, Ru-triphos based complexes have attracted attention as catalysts for the hydrogenation reactions of biomass derived products, such as levulinic acid,^{19,20} bio-esters^{11,21} and carbon dioxide²² to higher value chemicals. It would be advantageous to expand the scope of Ru-triphos derivatives that are either as, or more active than the systems already reported, especially if they are synthetically easier to access, such as the *N*-triphos ligand. The most studied carbon-centered analogue typically suffers from low yielding synthesis and involves highly air-sensitive metal phosphide reagents, unlike the *N*-triphos ligand, which is more adaptable and easier to prepare.¹⁰⁻¹⁸

N-triphos ligands remain relatively under-investigated, with only molybdenum, tungsten, ruthenium, rhodium and gold complexes having been reported from nine publications. This is in stark contrast to the boron- and carbon-centered analogues, for which there are around 50 and 900 articles, respectively, with a great number of unique compounds. Nonetheless, *N*-triphos containing complexes have found application in the asymmetric catalytic hydrogenation of pro-chiral olefins²³ as well as asymmetric cyclohydroamination of *N*-protected γ -allenyl sulfonamides.²⁴ Additionally, a ruthenium complex coordinated by a bulky *N*-triphos ligand featuring phospholane coordinating moieties was found to activate silanes, a key step in the development of organosilicon chemistry.²⁵

As part of the ongoing research program in catalysis, we sought to prepare a range of ruthenium *N*-triphos^{Ph} precatalysts and to investigate their stoichiometric reactions and catalytic potential. Despite molybdenum complexes of *N*-triphos^{Ph} having first been reported over 25 years ago, their application, catalytic or otherwise has not been investigated. This work demonstrates the applicability of the *N*-triphos scaffold, which

despite being generally underdeveloped, possess many desirable features such as complex stability. Herein we report the synthetic route and characterization of to a series of ruthenium *N*-triphos^{Ph} complexes that may find application in catalytic hydrogenation reactions.

Protocol

Note: Carry out all syntheses in a fume hood, and only after appropriate safety issues have been identified and measures taken to protect against them. Personal protective equipment include a lab coat, gloves and safety goggles and should be worn at all times.

1. Synthesis of *N,N,N*-tris(diphenylphosphinomethylene)amine, $N(\text{CH}_2\text{PPh}_2)_3$ (*N*-triphos^{Ph}) (1)

1. To a 200 ml oven dried Schlenk flask add diphenyl(hydroxymethylene)phosphonium chloride¹¹ (6.99 g, 24.7 mmol) and place under nitrogen via three sequential vacuum-nitrogen cycles on a dual-manifold Schlenk line.
2. Add degassed methanol (30 ml) and triethylamine (9.5 ml, 68.1 mmol), and stir at RT for 1 hr to ensure conversion of the phosphonium chloride salt to the hydroxymethene phosphine. Next, add degassed ammonia solution in methanol (2 M, 4.1 ml, 8.2 mmol).
3. Heat the reaction mixture for 2 hr under reflux, during which the ligand will precipitate out as a white solid.
4. Although the *N*-triphos^{Ph} ligand is stable to oxidation in air over short periods of time, for optimal purity, remove the solvent via cannula filtration²⁶ under nitrogen, and rinse with degassed methanol (3 x 10 ml) to obtain an analytically pure product, and store under a nitrogen atmosphere.

2. Synthesis of $[\text{Ru}(\text{CO})_2\{\text{N}(\text{CH}_2\text{PPh}_2)_3\}-\kappa^3\text{P}]$ (2)

1. To a 200 ml oven dried Schlenk flask, add *N*-Triphos^{Ph} (1.0 g, 1.63 mmol) and $[\text{Ru}_3(\text{CO})_{12}]$ (347 mg, 0.54 mmol), and place under nitrogen via three sequential vacuum-nitrogen cycles on a dual-manifold Schlenk line.
2. Add 30 ml of dry, degassed toluene and bring the mixture to reflux for 12 hr.
3. After this 12 hr reflux, filter the solution via cannula to a second Schlenk flask to remove small amounts of metallic ruthenium that form during the course of the reaction.
4. Reduce the volume of solvent to approximately 10 ml under vacuum using a dual-manifold Schlenk line fitted with a liquid nitrogen cooled trap, to induce precipitation of the complex.
5. Recrystallize the precipitate by heating gently (80–90 °C) in an oil bath until complete redissolution occurs, and subsequent slow cooling to RT by removing the heat from the oil bath, but allowing the Schlenk flask to remain submerged. Leave O/N to give an orange crystalline solid.
6. Isolate the orange crystals suitable for X-ray diffraction via cannula filtration of the supernatant into another oven dried Schlenk flask. Next, rinse the crystals with dry and degassed toluene (2 x 5 ml) and dry *in vacuo* O/N. Save the combined supernatant and washings in a separate Schlenk flask.
7. Obtain a second batch of crystals from the combined supernatant and rinsing solutions by a similar recrystallization process to steps 2.5 and 2.6 to improve the overall yield of reaction.
8. Store the complex under nitrogen as exposure to air leads to the slow conversion to the oxidized carbonate complex (see below).

3. Synthesis of $[\text{Ru}(\text{CO}_3)(\text{CO})\{\text{N}(\text{CH}_2\text{PPh}_2)_3\}-\kappa^3\text{P}]$ (3)

1. To a 200 ml Schlenk flask, add 2 (280 mg, 0.364 mmol) and 5 ml of toluene to generate a partially dissolved orange suspension.
2. Insert a needle attached to a balloon of oxygen into the suspension and bubble oxygen at a rate of 2–3 bubbles per second through the reaction mixture for 10 min.
3. As an orange precipitate forms, collect it by filtration in air and washed with toluene (2 x 5 ml) and diethyl ether (2 x 5 ml) and dry *in vacuo* to give a free flowing orange powder that was stable in air.
4. In order to grow crystals suitable for X-ray diffraction, dissolve 100 mg of 3 in 3 ml dichloromethane in a vial and layer 3 ml toluene on top by slowly allowing this solvent to run down the side of the vial.
 1. Leave this O/N to obtain crystals. Isolate the crystals by decanting the supernatant, and washing the toluene (2 x 3 ml) and diethyl ether (2 x 3 ml). Dry *in vacuo* on a dual-manifold Schlenk line.

4. Synthesis of $[\text{Ru}(\text{H})_2(\text{CO})\{\text{N}(\text{CH}_2\text{PPh}_2)_3\}-\kappa^3\text{P}]$ (4)

1. Prepare a solution of 3 (763 mg, 0.953 mmol) in 20 ml of dry, degassed THF and inject into a 100 ml Autoclave Engineer's high-pressure reactor under a positive pressure (0.2 bar) of nitrogen.
2. Change the reactor head space gas to 100% hydrogen and pressurize to 15 bar at RT, then heat to 100 °C with stirring for 2 hr.
Caution! *Ensure all safety procedures have been adhered to when using high pressure systems!*
3. After cooling to RT, carefully vent the excess hydrogen gas in the reactor head space and change to nitrogen.
4. Transfer the reaction solution to a 100 ml Schlenk flask under nitrogen and, after reconnecting to a dual-manifold Schlenk line, filter via cannula and dilute with 20 ml of dry, degassed methanol.
5. Remove the solvent under vacuum using a dual-manifold Schlenk line fitted with a liquid nitrogen cooled trap to give an orange powder. Wash this orange powder with dry, degassed methanol (3 x 5 ml) and dry, degassed diethyl ether (3 x 5 ml) and dry *in vacuo*.
6. Grow crystals suitable for X-ray diffraction analysis O/N from a saturated dry and degassed toluene solution of 4 layered with an equivolume amount of dry, degassed methanol.
7. Store the complex under nitrogen.

5. Reaction of $[\text{RuH}_2(\text{CO})\{\text{N}(\text{CH}_2\text{PPh}_2)_3\}-\kappa^3\text{P}]$ (4) with NH_4PF_6 and Levulinic Acid

1. Prepare a solution of 4 (48.4 mg, 65.2 μmol) in 2 ml dry, degassed toluene in a oven dried Schlenk flask, and add via syringe to a stirred solution of NH_4PF_6 (10.6 mg, 65.0 μmol) in acetonitrile (2 ml) in a separate oven dried Schlenk flask.
2. Stir the reaction mixture at RT for 2 hr. After, remove the solvent *in vacuo* using a dual-manifold Schlenk line fitted with a liquid nitrogen cooled trap to give the intermediate complex $[\text{RuH}(\text{CO})(\text{MeCN})\{\text{N}(\text{CH}_2\text{PPh}_2)_3\}-\kappa^3\text{P}]$ (5).
3. Wash with dry, degassed hexane (3 x 3 ml) and dry *in vacuo* to isolate complex 5 as a brown powder.
4. To a solution of 5 in 0.5 ml degassed acetone- d_6 , add levulinic acid (10.8 mg, 93.0 μmol , 1.43 equiv.) in 0.5 ml of degassed acetone- d_6 . Stir the reaction mixture for 2 min using a vortex stirrer.
5. Record ^1H and $^{30}\text{P}\{^1\text{H}\}$ NMR spectra of the reaction every hour for 16 hr to observe the reaction.²⁷

Representative Results

The *N*-triphos^{Ph} ligand (1) and the ruthenium complex series: $[\text{Ru}(\text{CO})_2\{\text{N}(\text{CH}_2\text{PPh}_2)_3\}-\kappa^3\text{P}]$ (2), $[\text{Ru}(\text{CO})_3(\text{CO})\{\text{N}(\text{CH}_2\text{PPh}_2)_3\}-\kappa^3\text{P}]$ (3) and $[\text{Ru}(\text{H})_2(\text{CO})\{\text{N}(\text{CH}_2\text{PPh}_2)_3\}-\kappa^3\text{P}]$ (4) were characterized via ^1H , $^{13}\text{C}\{^1\text{H}\}$, $^{30}\text{P}\{^1\text{H}\}$ NMR spectroscopy, FT-IR, ESI mass spectrometry and elemental analysis. Representative ^1H and $^{30}\text{P}\{^1\text{H}\}$ NMR data are shown in Table 1. In the case of complexes 2, 3 and 4 single crystal X-ray analysis unequivocally confirms their molecular structures. $^{30}\text{P}\{^1\text{H}\}$ NMR spectroscopy is a particularly useful technique for studying these complexes as characteristic shifts to higher frequency relative to free ligand and splitting patterns can be used to identify successful ligand coordination and identify particular geometries of complexes.

The free ligand *N*-triphos^{Ph} (1) displays a single resonance in the $^{30}\text{P}\{^1\text{H}\}$ NMR spectrum (CDCl_3 , 162 MHz) at -28.9 ppm. Occasionally, oxide peaks may appear at higher frequencies in the $^{30}\text{P}\{^1\text{H}\}$ NMR spectrum if due care is not take to exclude oxygen during the reaction or when making a solution for NMR spectroscopy. Reaction of *N*-triphos^{Ph} (1) with $[\text{Ru}_3(\text{CO})_{12}]$ results in the dicarbonyl complex $[\text{Ru}(\text{CO})_2\{\text{N}(\text{CH}_2\text{PPh}_2)_3\}-\kappa^3\text{P}]$ (2) that shows a characteristic higher frequency shift of a singlet to 8.3 ppm in the $^{30}\text{P}\{^1\text{H}\}$ NMR spectrum (C_6D_6 , 162 MHz), indicating that all the phosphine arms are coordinated to the Ru center and are in the same chemical environment. The X-ray crystal structure also confirmed this (Figure 4A).

Oxidation of 2 to gives the ruthenium(II) carbonate complex $[\text{Ru}(\text{CO})_3(\text{CO})\{\text{N}(\text{CH}_2\text{PPh}_2)_3\}-\kappa^3\text{P}]$ (3), simply by bubbling molecular oxygen through a suspension of 2 in toluene. A significant change in the $^{30}\text{P}\{^1\text{H}\}$ NMR spectrum is seen compared to 2. A characteristic triplet and doublet, AB₂ coupling pattern, is seen in the $^{30}\text{P}\{^1\text{H}\}$ NMR spectrum of 3 with resonances at -23.5 ppm (triplet) and 15.9 ppm (doublet) as there are now two different phosphorus environments, a result of the loss of symmetry on the formation of a carbonate. FT-IR can be used to confirm characteristic κ^2 -carbonate stretches at 1,565 and 1,434 cm^{-1} . Single crystal X-ray diffraction analysis also confirmed this structure (Figure 4B).

Hydrogenation of 3 under 15 bar hydrogen pressure gives the dihydrogen complex $[\text{Ru}(\text{H})_2(\text{CO})\{\text{N}(\text{CH}_2\text{PPh}_2)_3\}-\kappa^3\text{P}]$ (4) (Figure 2). The $^{30}\text{P}\{^1\text{H}\}$ NMR spectrum in C_6D_6 gave a doublet at 8.5 ppm and triplet at 18.8 ppm, indicating two different phosphorus environments. The ^1H NMR spectrum shows characteristic hydride resonances in the low frequency region of the spectrum as a multiplet centered around -6.50 ppm. Single crystal X-ray diffraction analysis also confirmed the structure of dihydride complex (Figure 4C).

Reaction of 4 with NH_4PF_6 in acetonitrile results in the loss of a hydride ligand and the formation of molecular H_2 , and $[\text{RuH}(\text{CO})(\text{MeCN})\{\text{N}(\text{CH}_2\text{PPh}_2)_3\}-\kappa^3\text{P}](\text{PF}_6)$ (5) (Figure 3). The $^{30}\text{P}\{^1\text{H}\}$ NMR spectrum is further complicated as there are now three different phosphorus environments owing to the three different *trans* ligands coordinating to the ruthenium center. A multiplet and two doublet-of-doublets at -12.4, 3.9 ppm and 26.5 ppm are seen (Figure 5). In the low frequency region of the ^1H NMR spectrum a pseudo doublet-of-triplets for 5 is seen at -6.3 ppm (Figure 6). The addition of levulinic acid to 5 gives the complex $[\text{Ru}(\text{CO})\{\text{N}(\text{CH}_2\text{PPh}_2)_3\}-\kappa^3\text{P}\{\text{CH}_3\text{CO}(\text{CH}_2)_2\text{CO}_2\text{H}\}-\kappa^2\text{O}](\text{PF}_6)$ (6) (Figure 3). The ^1H NMR spectrum of 6 after 21 hr shows the complete disappearance of the Ru-H signal (Figure 5) and $^{30}\text{P}\{^1\text{H}\}$ NMR spectrum shows a pseudo triplet at -16.2 ppm and doublet 19.8 ppm (Figure 6).

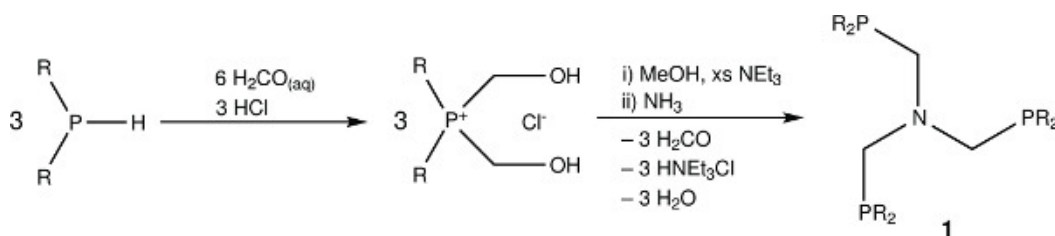


Figure 1. The chemical structures of the triphosphine ligand *N*-triphos^{Ph} and its generation synthetic scheme.

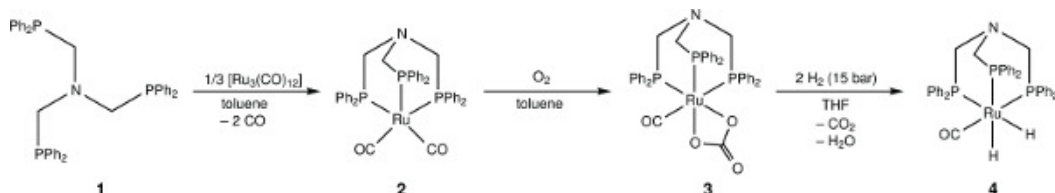


Figure 2. The chemical structure of ruthenium complexes of *N*-triphos^{Ph} and a synthetic scheme for their sequential preparation.

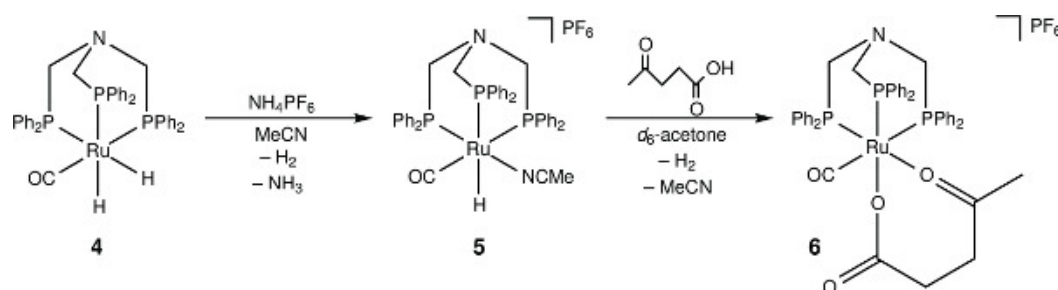


Figure 3. The activation of $[\text{RuH}_2(\text{CO})\{\text{N}(\text{CH}_2\text{PPh}_2)_3\}-\kappa^3\text{P}]$ with NH_4PF_6 and subsequent coordination with levulinic acid.

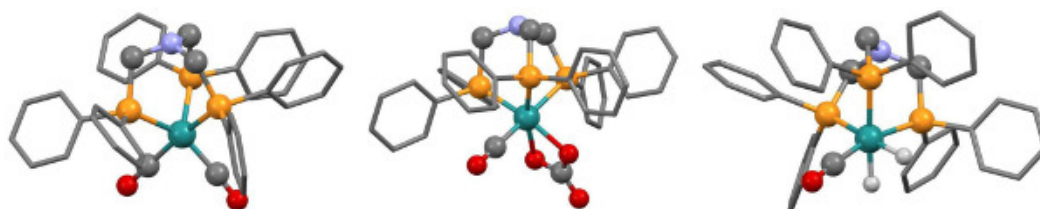


Figure 4. X-ray crystal structures of three Ru-N-triphos^{Ph} complexes, bearing (A) dicarbonyl (complex 2) (B) carbonate carbonyl (complex 3) and (C) dihydride (complex 4) ancillary ligands. These structures were obtained by Andrew J. P. White of Imperial College London. Note, crystals of $[\text{Ru}(\text{CO}_3)(\text{CO})\{\text{N}(\text{CH}_2\text{PPh}_2)_3\}-\kappa^3\text{P}]$ were found to contain two crystallographically independent complexes, only one of which is shown here. [Please click here to view a larger version of this figure.](#)

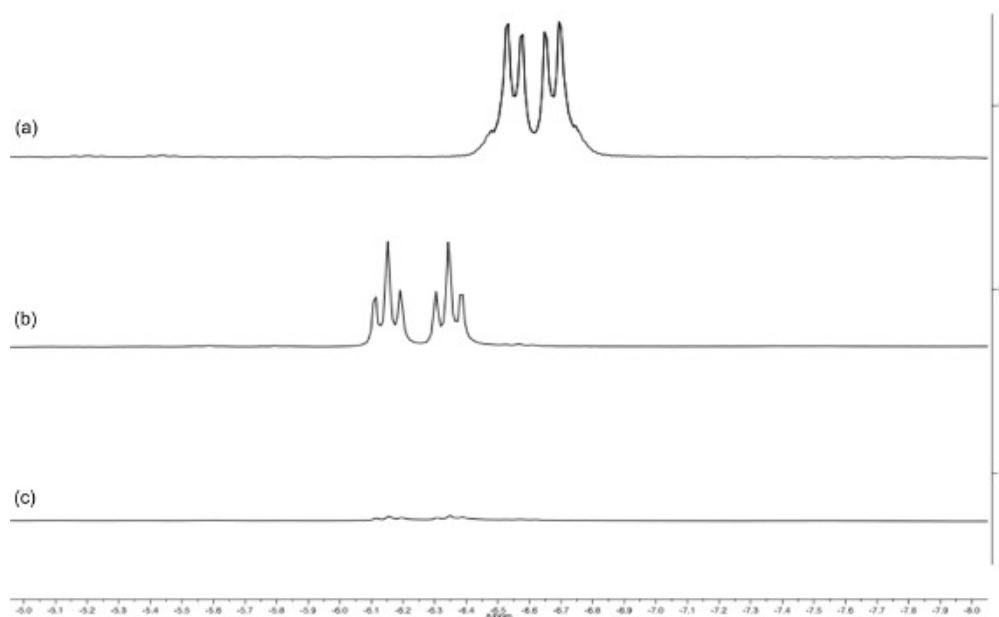


Figure 5. Stacked spectra of the hydride region (-5 to -8 ppm) of the ^1H NMR spectra of $[\text{RuH}_2(\text{CO})\{\text{N}(\text{CH}_2\text{PPh}_2)_3\}-\kappa^3\text{P}]$ (a, d_8 -toluene, 400 MHz), $[\text{RuH}(\text{CO})(\text{MeCN})\{\text{N}(\text{CH}_2\text{PPh}_2)_3\}-\kappa^3\text{P}]\text{PF}_6$ (b, d_6 -acetone, 400 MHz) and $[\text{Ru}(\text{CO})\{\text{N}(\text{CH}_2\text{PPh}_2)_3\}-\kappa^3\text{P}\{\text{CH}_3\text{CO}(\text{CH}_2)_2\text{CO}_2\text{H}\}-\kappa^2\text{O}]\text{PF}_6$ (c, d_6 -acetone, 400 MHz). Note the change as the complex is converted from a dihydride (pseudo doublet-of-doublets) to a monohydride (doublet-of-triplets) and finally to complete loss of hydride ligands.

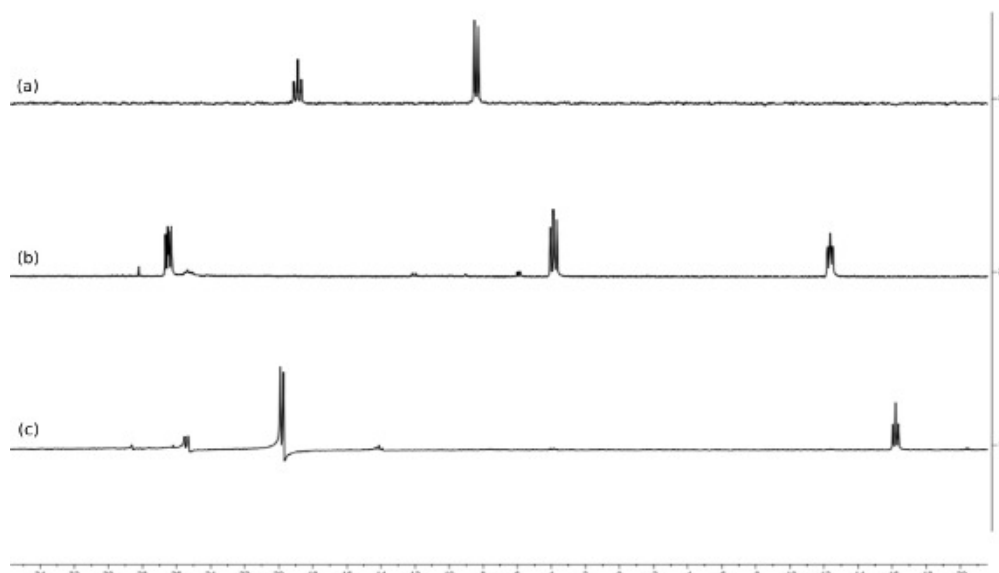


Figure 6. Stacked $^{30}\text{P}\{^1\text{H}\}$ spectra of $[\text{RuH}_2(\text{CO})(\text{N}(\text{CH}_2\text{PPh}_2)_3)-\kappa^3\text{P}]$ (a, d_8 -toluene, 162 MHz), $[\text{RuH}(\text{CO})(\text{MeCN})(\text{N}(\text{CH}_2\text{PPh}_2)_3)-\kappa^3\text{P}]\text{PF}_6$ (b, d_6 -acetone, 162 MHz) and $[\text{Ru}(\text{CO})(\text{N}(\text{CH}_2\text{PPh}_2)_3)-\kappa^3\text{P}\{\text{CH}_3\text{CO}(\text{CH}_2)_2\text{CO}_2\text{H}\}-\kappa^2\text{O}](\text{PF}_6)$ (c, d_6 -acetone, 162 MHz). Note how the splitting pattern and number of resonances changes with identity of the ancillary ligands.

Compound (solvent)	^1H & $^{30}\text{P}\{^1\text{H}\}$ peak assignment, chemical shift (ppm), splitting pattern and integration				
	NCH_2P	Ru-H	PPh_2		
$\text{N-triphos}^{\text{Ph}}$ (CDCl_3)	3.88, 6H, s	-	-28.9, 3P, s	-	-
$[\text{Ru}(\text{CO})_2(\text{N}(\text{CH}_2\text{PPh}_2)_3)-\kappa^3\text{P}]$ (C_6D_6)	3.93, 6H, s	-	8.25, 3P, s	-	-
$[\text{Ru}(\text{CO})_2(\text{CO})(\text{N}(\text{CH}_2\text{PPh}_2)_3)-\kappa^3\text{P}]$ (CDCl_3)	4.05 – 4.17, 6H, m	-	-23.5, 1P, t	15.9, 2P, d	-
$[\text{RuH}_2(\text{CO})(\text{N}(\text{CH}_2\text{PPh}_2)_3)-\kappa^3\text{P}]$ (C_6D_6)	3.66, 2H, s	3.82, 4H, m	-6.50, 2H, pseudo dd	8.53, 2P, d	18.8, 1P, t
$[\text{RuH}(\text{CO})(\text{MeCN})(\text{N}(\text{CH}_2\text{PPh}_2)_3)-\kappa^3\text{P}](\text{PF}_6)$ (d_6 -acetone)	-	-6.30, 1H, pseudo dt	-12.4, 1P, m	3.88, 1P, dd	26.5, 1P, dd
$[\text{Ru}(\text{CO})(\text{N}(\text{CH}_2\text{PPh}_2)_3)-\kappa^3\text{P}\{\text{CH}_3\text{CO}(\text{CH}_2)_2\text{CO}_2\text{H}\}-\kappa^2\text{O}](\text{PF}_6)$ (d_6 -acetone)	4.55 – 4.68, 6H, m	-	-16.2, 1P, pseudo t	19.8, 2P, pseudo d	-

Table 1. The ^1H and $^{30}\text{P}\{^1\text{H}\}$ NMR characterization data of the triphosphine ligand and subsequent ruthenium complexes. d = doublet, t = triplet, m = multiplet; pseudo splitting patterns are observed when two separate resonances have very similar chemical shifts and coupling constants.

Discussion

Herein we have described efficient synthetic procedures for the synthesis of a tridentate phosphine ligand and a series of ruthenium complexes. The $\text{N-triphos}^{\text{Ph}}$ ligand (**1**) can be easily prepared in high yield with a minimalistic work-up procedure. This phosphorus based Mannich reaction used to synthesize these types of ligands is quite general and can be used for other ligand derivatives with differing R-groups on the P-atoms.^{10-12,15-18} Additionally, this synthetic methodology is amenable to the analogous carbon-centered triphos ligand, and can be used to afford the same ruthenium dihydride species as with the N-triphos ligands. Previously, synthesis of these complexes required high temperatures and pressures, as well as long reaction times, which are negated in this procedure.

The synthesis of the series of ruthenium complexes **2**, **3**, **4**, **5** and **6** is performed in a linear fashion beginning with the chelation of $\text{N-triphos}^{\text{Ph}}$ **1** to $[\text{Ru}_3(\text{CO})_{12}]$ to generate the ruthenium dicarbonyl complex **2**. This dicarbonyl complex is then easily converted to the carbonate complex **3** via a simple oxidation procedure and conveniently isolated as an air stable solid. An oxidative process is of critical importance for the generation of hydride containing ruthenium species in this case. The central ruthenium atom in complex **2** is in the zero oxidation state, and the reductive conditions present during reaction with H_2 will not permit the necessary oxidation from ruthenium(0) to ruthenium(II) required in complex **4**.

Consequently, an initial oxidation is required. Chemical oxidants such as silver(I) salts can be used, and subsequent hydrogenation affords monohydride species,¹² however for the desired dihydride species, molecular oxygen must be used as the oxidant.

Complex **3** is converted to the dihydride complex **4**, which has potential uses in hydrogenation catalysis, a point to note here is that complex **4** is unstable in chlorinated solvents and will react over time to give mixtures of Ru-Cl species, hence NMR samples were typically run in C₆D₆. It was found that complex **4** needs to be activated with a proton source, in this case NH₄PF₆, to generate the active complex **5** before it will react with LA. **5** is found to react readily with LA over a 21-hr period can be conveniently monitored using ¹H and ³¹P{¹H} NMR spectroscopy. ¹H and ³¹P{¹H} NMR spectroscopy are particularly useful techniques for characterizing the complexes at each stage of the synthesis, as changes in ³¹P{¹H} splitting patterns and coupling constants provide important information about complex geometry (**Figure 6**) whilst ¹H NMR is able to detect the appearance and disappearance of characteristic hydride signals (**Figure 5**).

It is important that oxygen is excluded from reactions during the synthesis of **2**, **4**, **5** and **6**, as these complexes will react, normally into uncharacterizable decomposition products. Additionally, acetone-d₆ is required for observing the conversion of complex **5** to **6** by NMR spectroscopy. Deuterated solvents are required, as proton signals in non-deuterated solvents will interfere with those of the compound of interest during ¹H NMR spectroscopy. Acetone was chosen specifically as chlorinated solvents cannot be used, and other solvents such as THF will interfere with the reaction.

During oxidation from complex **2** to **3**, it is important not to over-oxidize the product, as this will lead to decomposition. The bubbling of oxygen through the suspension of **2** (step 3.2), should not be done for longer than around 10 min. Occasionally, a greenish byproduct is formed during the reaction, if this builds up significantly, the oxygen stream should be stopped and the solution purged by bubbling nitrogen through for 10 min. In small quantities, this byproduct is removed during the wash with diethyl ether (step 3.3). In general each complex (except for **6**) is stable in air for short periods when in the solid state, allowing it to be weighed without special precautions.

A limitation of this procedure is the requirement of a high-pressure system that allows the conversion of complex **3** to **4**. This is typically carried out at 15 bar H₂ pressure (step 4.2). This step has been carried out at higher pressures (up to 50 bar) however this was not found to increase yield or decrease reaction time. Although the synthesis has not been attempted at lower pressures in the lab, it is possible that conditions as mild as 1–2 bar would be sufficient. In this case, non-specialized equipment such as Young's tap sealed ampules could be used for this reaction. It should be noted that any pressurized system is highly dangerous and every measure should be taken to ensure the safety of the user and bystanders, and any required health and safety documentation is completed prior to the reaction.

Although a pressurized synthesis is still required to synthesize complex **4**, it remains more facile than the analogous, previously reported dihydride complex with the carbon-centered Triphos (rather than *N*-triphos^{Ph}). These reports required either harsh reaction conditions (120 bar H₂, 150 °C, 20 hr)²⁰ or several highly air-sensitive steps that require use of a nitrogen-filled glovebox.^{28,29} The reported method will allow the wider use of these species as they become more accessible to non-specialized groups. There are several possible future uses for these species, including but not limited to hydrogenation and hydrogenolysis catalysts, as well as catalysts for water splitting and hydrogen production. These will be useful for developing a sustainable future, at the heart of which, will almost certainly be chemical innovation.

Disclosures

The authors have nothing to disclose.

Acknowledgements

AP is grateful to Imperial College London for a PhD studentship via the Frankland Chair endowment. Johnson Matthey plc are also thanked for the loan of the precious metal salts used in this work.

References

- Bruneau, C., Dixneuf, P. H. *Ruthenium Catalysis and Fine Chemicals*. Springer New York (2004).
- Naota, T., Takaya, H., Murahashi, S. -L. Ruthenium-Catalyzed Reactions for Organic Synthesis. *Chem. Rev.* **98**, (7), 2599-2660 (1998).
- Arockaim, P. B., Bruneau, C., Dixneuf, P. H. Ruthenium(II)-Catalyzed C-H Bond Activation and Functionalization. *Chem. Rev.* **112**, (11), 5879-5918 (2012).
- Trost, B. M., Toste, F. D., Pinkerton, A. B. Non-metathesis ruthenium-catalyzed C-C bond formation. *Chem. Rev.* **101**, (7), 2067-2096 (2001).
- Vougioukalakis, G. C., Grubbs, R. H. Ruthenium-Based Heterocyclic Carbene-Coordinated Olefin Metathesis Catalysis. *Chem. Rev.* **110**, (3), 1746-1787 (2010).
- Lozano-Vila, A. M., Monsaert, S., Bajek, A., Verpoort, F. Ruthenium-based olefin metathesis catalysts derived from alkynes. *Chem. Rev.* **110**, (8), 4865-4909 (2010).
- Samojlowicz, C., Bieniek, M., Grela, K. Ruthenium-based olefin metathesis catalysts bearing N-heterocyclic carbene ligands. *Chem. Rev.* **109**, (8), 3708-3742 (2009).
- Alcaide, B., Almedros, P., Luna, A. G. rubbs' Ruthenium-Carbenes Beyond the Metathesis Reaction: Less Conventional Non-Metathetic Utility. *Chem. Rev.* **109**, (8), 3817-3858 (2009).
- Conley, B. L., Pennington-Boggio, M. K., Boz, E., Discovery Williams, T. J. Applications, and Catalytic Mechanisms of Shvo's Catalyst. *Chem. Rev.* **110**, (4), 2294-2312 (2010).
- Miller, P. W., White, A. J. P. The preparation of multimetallic complexes using sterically bulky N-centered tipodal dialkyl phosphine ligands. *J. Organomet. Chem.* **695**, (8), 1138-1145 (2010).
- Hanton, M. J., Tin, S., Boardman, B. J., Miller, P. Ruthenium-catalysed hydrogenation of esters using tripodal phosphine ligands. *J. Mol. Catal. A.* **346**, (1-2), 70-78 (2012).

12. Phanopoulos, A., Brown, N. J., White, A. J. P., Long, N. J., Miller, P. W. Synthesis, Characterization, and Reactivity of Ruthenium Hydride Complexes of N-Centered Triphosphine Ligands. *Inorg. Chem.* **53**, (7), 3742-3752 (2014).
13. Jin, G. Y. N.N.N'-tris(phosphinomethylen)amine N.N.N'-tris(phosphinomethylene)hydrazine N.N.N'.N'-tetra(phosphinomethylene)hydrazine. *Tetrahedron Lett.* **22**, (12), 1105-1108 (1981).
14. Walter, O., Huttner, G., Kern, R. Preparation and Characterisation of $N(CH_2PPh_2)_3$. $N(CH_2PPh_2)_3Mo(CO)_3$ and $[HN(CH_2PPh_2)_3Mo(CO)_3]BF_4$. *Z. Naturforsch.* **51b**, 922-928 (1996).
15. Fillol, J. L., Kruckenberg, A., Scherl, P., Wadepohl, H., Gade, L. H. Stitching Phospholanes Together Piece by Piece: New Modular Di- and Tridentate Stereodirecting Ligands. *Chem. Eur. J.* **17**, (50), 14047-14062 (2011).
16. Rodríguez, L. -I., Roth, T., Fillol, J. L., Wadepohl, H., Gade, L. H. The More Gold–The More Enantioselective: Cyclohydroaminations of γ -Allenyl Sulfonamides with Mono Bis-, and Trisphospholane Gold(I) Catalysts. *Chem. Eur. J.* **18**, (12), 3721-3728 (2012).
17. Scherl, P., Kruckenberg, A., Mader, S., Wadepohl, H., Gade, L. H. Ruthenium η^4 -Trimethylenemethane Complexes Containing Tripodal Phosphanomethylamine Ligands. *Organometallics*. **31**, (19), 7024-7027 (2012).
18. Scherl, P., Wadepohl, H., Gade, L. H. Hydrogenation and Silylation of a Double-Cyclometalated Ruthenium Complex: Structures and Dynamic Behavior of Hydrido and Hydridosilicate Ruthenium Complexes. *Organometallics*. **32**, (15), 4409-4415 (2013).
19. Geilen, F. M. A. Selective and Flexible Transformation of Biomass-Derived Platform Chemicals by a Multifunctional Catalytic System. *Angew. Chem. Int. Ed.* **49**, (32), 5510-5514 (2010).
20. Geilen, F. M. A., Engendahl, B., Hölscher, M., Klankermayer, J., Leitner, W. Selective Homogeneous Hydrogenation of Biogenic Carboxylic Acids with $[Ru(TrisPhos)H]^+$: A Mechanistic Study. *J. Am. Chem. Soc.* **133**, (36), 14349-14358 (2011).
21. Van Engelen, M. C., Teunissen, H. T., de Vries, J. G., Elsevier, C. J. Suitable ligands for homogeneous ruthenium-catalyzed hydrogenolysis of esters. *J. Mol. Catal. A.* **206**, (1-2), 185-192 (2003).
22. Wesselbaum, S., vom Stein, T., Klankermayer, J., Leitner, W. Hydrogenation of Carbon Dioxide to Methanol by Using a Homogeneous Ruthenium–Phosphine Catalyst. *Angew. Chem. Int. Ed.* **51**, (30), 7499-7502 (2012).
23. Fillol, J. L., Kruckenberg, A., Scherl, P., Wadepohl, H., Gade, L. H. Stitching Phospholanes Together Piece by Piece: New Modular Di- and Tridentate Stereodirecting Ligands. *Chem. Eur. J.* **17**, (50), 14047-14062 (2011).
24. Rodríguez, L. -I., Roth, T., Fillol, J. L., Wadepohl, H., Gade, L. H. The More Gold–The More Enantioselective: Cyclohydroaminations of γ -Allenyl Sulfonamides with Mono Bis-, and Trisphospholane Gold(I) Catalysts. *Chem. Eur. J.* **18**, (12), 3721-3728 (2012).
25. Scherl, P., Wadepohl, H., Gade, L. H. Hydrogenation and Silylation of a Double-Cyclometalated Ruthenium Complex: Structures and Dynamic Behavior of Hydrido and Hydridosilicate Ruthenium Complexes. *Organometallics*. **32**, (15), 4409-4415 (2013).
26. Bennett, B. K., Richmond, T. G. An Inexpensive, Disposable Cannula Filtration Device. *J. Chem. Educ.* **75**, (8), 1034 (1998).
27. Judd, C. S. Proton NMR Basics. *J. Chem. Educ.* **72**, (8), 706 (1995).
28. Rhodes, L. F., Venanzi, L. M. Ruthenium(II)-Assisted Borohydride Reduction of Acetonitrile. *Inorg. Chem.* **26**, (16), 2692-2695 (1987).
29. Bakhmutov, V. I. In-depth NMR and IR study of the proton transfer equilibrium between $[MeC(CH_2PPh_2)_3Ru(CO)H_2]$ and hexafluoroisopropanol. *Can. J. Chem.* **79**, 479-489 (2001).